College of Polymer Science and Polymer Engineering

8-8-2008

Partial Crystallinity in Alkyl Side Chain Polymers Dictates Surface Freezing

Shishir Prasad

Zhang Jiang

Sunil K. Sinha

Ali Dhinojwala
University of Akron Main Campus, ali4@uakron.edu

Recommended Citation

P H Y S I C A L   R E V I E W   L E T T E R S

Partial Crystallinity in Alkyl Side Chain Polymers Dictates Surface Freezing

Shishir Prasad,[1] Zhang Jiang,[2] Sunil K. Sinha,[2] and Ali Dhinojwala[1],*

[1]*Department of Polymer Science, The University of Akron, Akron, Ohio 44325, USA*
[2]*Department of Physics, University of California San Diego, La Jolla, California 92093, USA*

We have studied the structure of a novel crystalline surface monolayer on top of a disordered melt of the same material [poly(*n*-alkyl acrylate)s] using grazing incidence x-ray diffraction. The grazing incidence x-ray diffraction, surface tension, and bulk latent heat results show that side chains crystallize except the nine methylene units of the alkyl side chains closest to the polymer backbone. The partial crystallinity along with a thicker surface layer, due to the additional length of the linker group, explains why the difference between the surface order-to-disorder transition temperature and bulk melting temperature increases with a decrease in the length of the alkyl side chain.

Molecules at surfaces of most liquids have higher entropy and lower melting temperature (T_s) than in the bulk (T_m) [1]. Examples of these materials include macromolecules, organic liquids, metals, and even water. However, several exceptions have been discovered in the past two decades. Linear *n*-alkanes exhibit surface freezing, where the surfaces remain crystalline 1–3 K [$\Delta T = (T_s - T_m)$] above T_m [2,3]. This surface freezing has also been observed in several alkane derivatives such as alcohols, semifluorinated alkanes, alkenes, and surfactants at oil-water interface [4,5]. Interestingly, chemical attachment of alkyl chains using an acrylate linker group to a flexible polymeric backbone [poly(*n*-alkyl acrylate)s shown in Fig. 1(a)] leads to a dramatic increase in ΔT (≈ 9–20 K) [6]. The surfaces of these polymers exhibit a two-step transition from ordered-to-disordered state upon heating. The first transition involves a phase change from crystal to smecticlike surface monolayer at T_{s1}, ≈ 1–2 K higher than T_m. The second step is at T_{s2} (≈ 9–20 K above T_m) and is due to a transition from the smecticlike to disordered surface layer. Poly(*n*-alkyl acrylate)s were first synthesized in the late 1950s and are extensively used as release liners in pressure sensitive tapes, binder in cosmetic and personal care, smart adhesive, seed coating, and breathable packaging film [7]. The understanding of these novel surface phases provides opportunities to control the surface properties without affecting the bulk properties.

In this Letter, we unequivocally show by grazing incidence x-ray diffraction (GIXD) measurements that not all of the methylene groups of a surface side chain crystallize. We find that the length of the noncrystalline part of a side chain is constant (≈ 9 methylene groups) for side chain lengths of $n = 16$, 18, and 22. This partial crystallinity along with the presence of the linker group explains why ΔT is higher for poly(*n*-alkyl acrylate)s and why ΔT decreases as we increase the length of the side chain, a result which is very different for *n*-alkanes of similar chain lengths.

GIXD provides information on in-plane structure of molecules next to surfaces or interfaces. In GIXD measurements, the x-ray beam is incident on the surface with incident angles less than, or near, the critical angle for total external reflection (α_c). In this condition, the evanescent waves travel parallel to the surface and are most sensitive in probing the top 50–100 Å of the surface. The incident, reflection, and scattering angles are defined in Fig. 1(b). The scattering wave vector $\mathbf{q} = \mathbf{k}_f - \mathbf{k}_i$, where the wave vector of the incident radiation is identified by $\mathbf{k}_i$ and that of the scattered radiation by $\mathbf{k}_f$. q_z and q_r are wave-vector components in the z and radial direction, respectively. The scattered intensity along q_z at $q_r = 2\pi/d$ (d is the in-plane lattice spacing) is sensitive to the orientation and length (D) of the crystal structure normal to the surface. The wave vector in molecular coordinates is denoted by $\mathbf{Q}$. Therefore, Q_z (or Q_r) is the wave-vector component along (or normal) to the molecular axis. The intensity of scattered wave is given as [8,9]

$$I(q_z) \propto |T(\alpha_i)|^2 |T(\alpha_f)|^2 \left[\left(\frac{\sin(Q_z D/2)}{Q_z D/2} \right)^2 \right]. \quad (1)$$

$T(\alpha_i)$ and $T(\alpha_f)$ are the Fresnel coefficients of the incident and reflected field, respectively. The fit to x-ray intensity along q_z (at q_r equal to $2\pi/d$) using Eq. (1) determines the
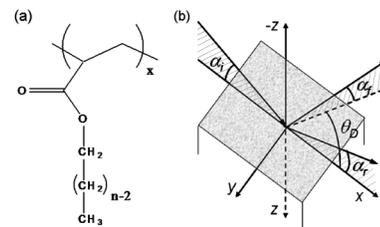
FIG. 1.   (a) The chemical structure of poly(*n*-alkyl acrylate), where $n = 16$, 18, and 22. (b) The schematic geometry of the x-ray experimental setup. The angle of incidence is α_i, the reflection angle is α_r, and the scattering angle is α_f.

crystal thickness (D) and its tilt (θ) with respect to the surface normal. When the surface molecules are aligned normal to the surface plane, $Q_z = q_z$, $Q_r = q_r$, and $\theta = 0$. In order to account for the curvature of the Bragg rods seen in the detector, Eq. (1) must be folded with a tilt distribution of molecular axes about the surface normal. This was carried out numerically, assuming an isotropic Gaussian distribution for the tilt angle, which turned out to have a width of $\leq 10°$. This is still small enough that it did not significantly change the intensity distribution along the q_z direction [see inset in Fig. 2(b)].

Poly(n-alkyl acrylate)s ($n = 16$: $T_m = 308.2$ K and $T_{s2} = 320.0$ K; $n = 18$: $T_m = 320.7$ K and $T_{s2} = 329.8$ K; and $n = 22$: $T_m = 336.5$ K and $T_{s2} = 344.0$ K) were obtained from Landec Corporation. The polydispersity (PD) of these polymers was broad (≈ 10–20; $M_n \approx 15\,000$ g mol^{-1}) due to the melt polymerization process. The results were consistent with the narrower PD polymers prepared by transesterification of poly(*tert*-butyl acrylate) having a PD of 1.12 with an alcohol of appropriate chain length [6]. GIXD experiments were performed on thin films (100–150 nm) of poly(n-alkyl acrylate)s coated on silicon wafers or glass slides. Films were prepared by spin coating 4–6 wt% polymer solution in toluene and subsequently annealing in a vacuum oven at 10 K above their respective T_{s2} for 4–5 h.

GIXD measurements were performed at the Advanced Photon Source (APS) (beam lines MuCAT and 1-BM) using a synchrotron radiation of wavelength (λ) 0.7684 Å at MuCAT and 1.0253 Å at 1-BM. In these experiments, the angle of incidence was set below α_c. The scattered x-ray

beam was imaged using a plate detector (resolution of 150 μm/pixel at MuCAT and 78.64 μm/pixel at 1-BM). All images from a sample were acquired with a constant exposure time. The diffraction from silicon powder was used to calibrate the distance between the sample and the detector plate. This calibration was then used to determine the angles α_f and θ_D [Fig. 1(b)].

Figure 2(a) shows the image of GIXD diffraction pattern on the CCD plate detector collected at temperatures just above T_m for poly(n-alkyl acrylate) with $n = 16$, 18, and 22. The presence of a crystalline surface layer is evident by the bright equatorial bands in Fig. 2(a), which are the Bragg rods from the surface crystalline phase. The Bragg rods are slightly curved due to tilting ($\leq 10°$) of the surface crystalline grains with respect to the surface normal. The diffraction pattern did not change upon azimuthal in-plane rotation of the films, indicating that the sample was polycrystalline with random grain orientations in the surface plane. The Bragg rods disappear on further increase in temperature even though the surface remains ordered [6]. The position of this Bragg peak corresponds to an in-plane lattice spacing of 4.2 Å. This lattice spacing is similar to that measured for the bulk crystals [10], indicating similarity in the chain packing at the surface and in the bulk. Assuming hexagonal packing in the surface layer as in the bulk crystal phase, we can determine the average spacing of 20.4 Å^2/side chain in the surface layer. These numbers are similar to those obtained for the surface crystalline phases of n-alkanes and alcohols [4,9].

Figures 2(b)–2(d) show the x-ray intensity along the Bragg rod as a function of α_f/α_c in the surface crystalline phase for poly(n-alkyl acrylate)s with side chain lengths of $n = 16$, 18, and 22, respectively. The scans were obtained by accumulating pixels with a constant abscissa of q_r corresponding to the in-plane lattice spacing of 4.2 Å (the intensity dropoffs along the arc were similar). The sharp peak at $\alpha_f/\alpha_c = 1$ is explained by the distorted wave Born approximation. This sharp peak rides on a second broad peak having maximum intensity at $\alpha_f = 0$, suggesting that the surface side chains are aligned perpendicular to the surface grains. The solid lines in Figs. 2(b)–2(d) are fits to the scans with Eq. (1) to obtain the thickness (D) of the surface crystalline phase. We have also plotted as dashed lines in Figs. 2(b)–2(d) the calculated intensity profiles expected for the surface crystal of thickness equal to an all-*trans* alkyl side chain. The intensity of the broad peak does not drop off as rapidly as expected based on the assumption that all of the methylene (including terminal methyl) groups of a surface side chain take part in crystallization. The best fit obtained for the surface crystal thickness suggests partial crystallinity of the side chains. The thickness of the surface crystal, the length of an all-*trans* alkyl side chain, and the average number of methylene groups in a side chain not taking part in surface crystallization (x_{GIXD}) are provided in Table I. Interestingly, the number of noncrystalline methylene groups of a surface
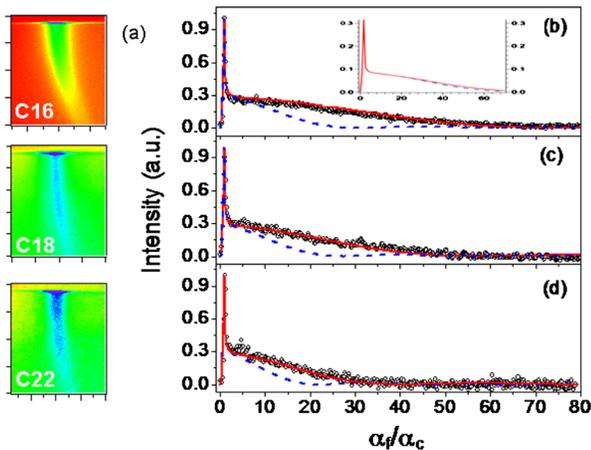
FIG. 2 (color online). (a) Image of diffraction pattern on a plate detector for poly(n-alkyl acrylate) in the surface crystalline phase ($T_m < T < T_{s1}$). The x-ray intensities along the Bragg rods for $n = 16$ (b), 18 (c), and 22 (d) are plotted as a function of α_f/α_c. Shown as solid lines are fits to the data using Eq. (1). The dashed lines indicate calculated intensity profiles for $D =$ extended side chain length. The inset in (b) compares the intensity dropoff along the arc (solid line) and along constant q_r (dashed line) for a Gaussian distribution with $\sigma = 8°$ tilt, $D = 8$ Å, and correlation length of 100 Å.

PHYSICAL REVIEW LETTERS

TABLE I. The thickness of surface crystalline phase [D in Eq. (1)] obtained by fitting the x-ray intensity along the Bragg rod (resolution of 0.5 Å) [Figs. 2(b)–2(d)], the calculated length of the all-*trans* alkyl side chain (L) (without the acrylate linker group), and the number of methylene units not taking part in crystallization [$x_{GIXD} = (L - D)/1.27$] are provided for $n = 16$, 18, and 22.

Polymer, n	D (Å)	All-*trans* side chain length (Å)	x_{GIXD}
16	7.9	19.3	9.0
18	10.5	21.9	8.9
22	15.0	26.9	9.4

side chain is constant (≈ 9). Since by surface sensitive infrared-visible nonlinear optical spectroscopy (SFG) we have observed high orientational order of terminal methyl groups, we can conclude that the units that are not crystalline are the ones closest to the polymer backbone [11]. Partial crystallinity of side chains in the bulk crystal was also inferred by Jordan *et al.* based on differential scanning calorimetry (DSC) measurements [12]. The number of noncrystalline methylene groups in a side chain in the bulk crystal was determined to be 9.2, in agreement with the GIXD results for the surface monolayer.

We now compare the GIXD results with surface tension and latent heat measurements. The slope of surface tension as a function of temperature ($d\gamma/dT$) is equal to the difference in bulk and surface entropy [13]. In the surface ordered phase, this slope [$(d\gamma/dT)_{T<T_{s2}}$] is positive (Table II) and changes sharply to a negative value (≈ -0.11 mN m^{-1} K^{-1}) with an increase in temperature at T_{s2} [14]. The change in entropy of the surface molecules upon disordering is equal to the difference in the slope of surface tension below and above T_{s2} [$= \Delta(d\gamma/dT)$]. We have tabulated $\Delta(d\gamma/dT)$ for poly(n-alkyl acrylate)s [$n = 16$, 18, and 22] in Table II. Since no change in ($d\gamma/dT$) was observed at T_{s1}, the entropy difference between the crystal and smecticlike phases must be small. This assumption is also supported by the SFG results which indicated all-trans oriented alkyl side chains below T_{s2} [11]. Therefore, $\Delta(d\gamma/dT)$ values in Table II correspond to the change in entropy of the surface phase as it undergoes a transition from an ordered to a disordered state.

TABLE II. $\Delta\gamma$ [$= (\gamma_{T_{s2}} - \gamma_{T_m})$], $(d\gamma/dT)_{T<T_{s2}}$, $\Delta(d\gamma/dT)$, and ΔS_b for $n = 16$, 18, and 22 measured in the heating cycle for poly(n-alkyl acrylate)s are provided. We have also tabulated the calculated values of $k_B \ln(3^{n-9}) \times 10^3/(20.4 \times 10^{-20})$ [$= \Delta(d\gamma/dT)_{calc}$] for different side chain lengths. $\Delta\gamma$ has units of mN m^{-1}. $(d\gamma/dT)_{T<T_{s2}}$, $\Delta(d\gamma/dT)$, ΔS_b, and $\Delta(d\gamma/dT)_{calc}$ values are reported in units of mN m^{-1} K^{-1}.

n	$\Delta\gamma$	$(d\gamma/dT)_{T<T_{s2}}$	$\Delta(d\gamma/dT)$	ΔS_b	$\Delta(d\gamma/dT)_{calc}$
16	4.6	0.46	0.59	0.51	0.52
18	5.1	0.57	0.68	0.64	0.67
22	6.6	0.89	0.98	0.88	0.97

Approximating the side chains in the surface melt to be completely flexible so that each bond conformation is of equal probability, the extra conformational entropy per side chain in the melt surface compared to that in the surface ordered phase is $k_B \ln(3^{n-x})$. Here x is the number of methylene groups per side chain that do not crystallize. In the crystalline state, the part of the side chain having reduced entropy due to surface ordering has only one conformation, i.e., *trans*, and hence possesses zero entropy [$= k_B \ln(1^{n-x})$]. Therefore, the difference in entropy between the disordered and crystal surface states is equal to $k_B \ln(3^{n-x}) \times 10^3/(20.4 \times 10^{-20})$ mN m^{-1} K^{-1}. The division factor of 20.4×10^{-20} is due to the unit conversion from per molecule to per unit area and is determined from GIXD measurements. The calculated difference in entropy between the disordered and crystal surface layer using a value of $x = 9$ agrees well with the experimentally obtained $\Delta(d\gamma/dT)$ and values calculated using bulk DSC measurements (ΔS_b) (Table II).

We have shown previously that the positional entropy loss due to the attachment of alkyl side chains to the acrylate backbone is very small [14]. The main differences between small molecule alkanes and poly(n-alkyl acrylate)s are the observation of partial crystallinity in the side chain polymers and higher values of $\Delta\gamma$ (defined below). ΔT can be written as [14]

$$\Delta T = \frac{\gamma_{T_{s2}} - \gamma_{T_m}}{\Delta(d\gamma/dT) + (d\gamma/dT)_{T>T_{s2}}}. \quad (2)$$

The slope of surface tension in the surface melt phase $(d\gamma/dT)_{T>T_{s2}} \approx$ constant $(= -0.11$ mN m^{-1} K^{-1}) for poly(n-alkyl acrylate)s. This slope is similar to $(d\gamma/dT)_{T>T_{s,alk}}$ for n-alkanes $(= -0.09$ mN m^{-1} K^{-1}) [9]. Here $T_{s,alk}$ is the surface disordering temperature of n-alkanes. A similar expression to Eq. (2) can be given for ΔT in n-alkanes by replacing T_{s2} with $T_{s,alk}$. ΔT depends on both $\Delta\gamma$ and the change in entropy upon ordering. We have listed $\Delta\gamma$ determined from the surface tension scans for three polymers with different side chain lengths in Table II.

When compared to n-alkanes [9], $\Delta\gamma$ is higher and the slope of surface tension in the surface ordered phase [$(d\gamma/dT)_{T<T_{s2}}$] is lower for poly(n-alkyl acrylate)s (Table II), leading to higher values of ΔT for polymers than that for n-alkanes [Eq. (2)]. This explains the increase in ΔT upon connecting n-alkanes to a polymer backbone using acrylate linkage. Under the assumption that the dominant missing interaction for the terminal methyl groups on the surface with the underlying bulk is given by van der Waals interaction, the excess free energy at T_m varies as $1/l^2$, where l is the thickness of the surface ordered phase. In the case of n-alkanes, $\gamma_{T_m} = (22.0 + 1200/n_{eff}^2)$ mN m^{-1} [3]. Here n_{eff} is the thickness of the surface ordered phase in units of the number of methylene groups in n-alkane. The value of l in poly(n-alkyl acrylate)s is higher than the corresponding n-alkane because of
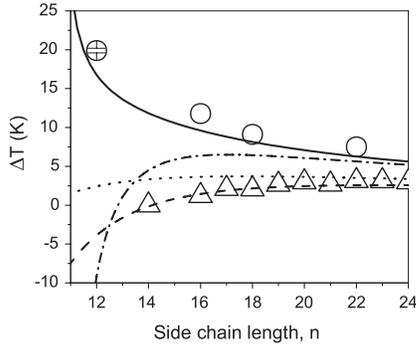
FIG. 3. The experimental values of ΔT for poly(n-alkyl acrylate)s ($\bigcirc$) [11,14] as a function of n. The predictions of ΔT using Eq. (2) are plotted after taking into consideration only the contribution of the extra length of the linker group in the surface ordered phase (dotted line) or the partial crystallinity of the surface side chains (dashed-dotted line). The predictions after taking into account both of these contributions are plotted as a solid line. We have also plotted the data for n-alkane ($\triangle$) and predictions (dashed line) for comparison [using $\gamma_{T_{s,\text{alk}}} = 28$ mN m^{-1}, $\gamma_{T_m} = (22 + 1200/n^2)$ mN m^{-1}, and $(d\gamma/dT)_{T < T_{s,\text{alk}}} = [k_B \ln(3^{n-3}) \times 10^3/(19.7 \times 10^{-20}) - 0.09]$ mN m^{-1} K^{-1}] [9].

the additional length of the linker group in the surface ordered phase, as revealed by x-ray reflectivity measurements [6]. In the case of poly(n-alkyl acrylate)s, the x-ray reflectivity fits matched the experimental data only after using the combined thickness of the alkyl part of the side chain and the acrylate linker group. Therefore, $n_{\text{eff}} = (n + 2.9)$, where 2.9 is the additional contribution of the linker group in units of the number of methylene groups. This suggests a lower surface tension at T_m for poly(n-alkyl acrylate)s than the corresponding n-alkanes. Furthermore, $\gamma_{T_{s2}}$ is found to be constant for $n = 16$, 18, and 22 ($\gamma_{T_{s2}} \approx$ constant $= 29.3$ mN m^{-1}) [14], similar to the observations for n-alkanes ($\gamma_{T_{s,\text{alk}}} = 28$ mN m^{-1}) [9]. Lower values of γ_{T_m} and higher values of γ_{T_s} lead to higher $\Delta\gamma$ for polymers compared to n-alkanes.

Since all parameters in Eq. (2) are now known [i.e., $\gamma_{T_{s2}} = 29.3$ mN m^{-1}, $\gamma_{T_m} = [22.0 + 1200/(n + 2.9)^2]$ mN m^{-1}, $\Delta(d\gamma/dT)_{\text{calc}} = k_B \ln(3^{n-9}) \times 10^3/(20.4 \times 10^{-20})$ mN m^{-1} K^{-1}, and $(d\gamma/dT)_{T > T_{s2}} = -0.11$ mN m^{-1} K^{-1}], ΔT can be calculated as a function of the side chain lengths. The calculated values of ΔT are shown in Fig. 3 as a solid line. Shown also in Fig. 3 are the data of ΔT for poly(n-alkyl acrylate)s [11,14] and n-alkanes [9]. The calculated results are in good agreement with the experimental values for poly(n-alkyl acrylate)s. For comparison, we have also plotted the expected trends in Fig. 3 if we consider only either the entropic or $\Delta\gamma$ contribution in Eq. (2) for poly(n-alkyl acrylate)s. The disagreement between these predictions and the experimental results clearly suggests that both the extra thickness of the linker group and the partial crystallinity in the

surface ordered phase are necessary to explain the experimental results. In comparison, the calculated values for n-alkanes (dashed line in Fig. 3) based on the hypothesis that the complete chain participates in the surface frozen layer is in agreement with the experimental data.

We have studied the surface frozen monolayer in poly(n-alkyl acrylate)s using grazing incidence x-ray diffraction. The GIXD results indicate that the surface side chains crystallize except the nine methylene units of the alkyl side chains closest to the polymer backbone. The partial crystallinity of the side chains and the additional length of the acrylate linker group successfully explains the trend of ΔT as a function of side chain length. These results provide important guidelines to modify the surface ordering temperatures by tailoring the length and flexibility of the side chain linker groups.

*ali4@uakron.edu
[1] H. Dosch, *Critical Phenomena at Surfaces & Interfaces* (Springer-Verlag, Berlin, 1992), 1st ed.
[2] J. C. Earnshaw and C. J. Hughes, Phys. Rev. A **46**, R4494 (1992).
[3] X. Z. Wu, B. M. Ocko, E. B. Sirota, S. K. Sinha, M. Deutsch, B. H. Cao, and M. W. Kim, Science **261**, 1018 (1993).
[4] O. Gang, X. Z. Wu, B. M. Ocko, E. B. Sirota, and M. Deutsch, Phys. Rev. E **58**, 6086 (1998).
[5] Q. Lei and C. D. Bain, Phys. Rev. Lett. **92**, 176103 (2004).
[6] K. S. Gautam, S. Kumar, D. Wermeille, D. Robinson, and A. Dhinojwala, Phys. Rev. Lett. **90**, 215501 (2003).
[7] D. J. Kinning, J. Adhes. **60**, 249 (1997).
[8] J. A. Nielsen and K. Kjaer, *Phase Transitions in Soft Condensed Matter* (Plenum, New York, 1989).
[9] B. M. Ocko, X. Z. Wu, E. B. Sirota, S. K. Sinha, O. Gang, and M. Deutsch, Phys. Rev. E **55**, 3164 (1997).
[10] N. A. Platé and V. P. Shibaev, Macromol. Rev. **8**, 117 (1974).
[11] K. S. Gautam and A. Dhinojwala, Phys. Rev. Lett. **88**, 145501 (2002).
[12] J. Jordan, F. Edmund, D. W. Feldeisen, and A. N. Wrigley, J. Polym. Sci., Part A: Polym. Chem. **9**, 1835 (1971).
[13] R. Defay and I. Prigogine, *Surface Tension and Adsorption* (Wiley, New York, 1966).
[14] S. Prasad, L. Hanne, and A. Dhinojwala, Macromolecules **38**, 2541 (2005).